Julie Gale

Journal of Neurochemistry
Lippincott Williams & Wilkins, Inc., Philadelphia

PA 1Aug2/001754

Characterization of Copper Interactions with Alzheimer Amyloid β Peptides: Identification of an Attomolar-Affinity Copper Binding Site on Amyloid β1–42

*†‡Craig S. Atwood, *†‡Richard C. Scarpa, *†‡Xudong Huang, ‡§Robert D. Moir, *†‡Walton D. Jones, ‖David P. Fairlie, ‡§Rudolph E. Tanzi, and *†‡Ashley I. Bush

**Laboratory for Oxidation Biology, Departments of †Psychiatry and §Neurology, and ‡Genetics and Aging Unit, Massachusetts General Hospital and Harvard Medical School, Boston, Massachusetts, U.S.A.; and ‖Centre for Drug Design and Development, University of Queensland, Brisbane, Queensland, Australia*

Abstract: Cu and Zn have been shown to accumulate in the brains of Alzheimer's disease patients. We have previously reported that Cu^{2+} and Zn^{2+} bind amyloid β (Aβ), explaining their enrichment in plaque pathology. Here we detail the stoichiometries and binding affinities of multiple cooperative Cu^{2+}-binding sites on synthetic Aβ1–40 and Aβ1–42. We have developed a ligand displacement technique (competitive metal capture analysis) that uses metal–chelator complexes to evaluate metal ion binding to Aβ, a notoriously self-aggregating peptide. This analysis indicated that there is a very-high-affinity Cu^{2+}-binding site on Aβ1–42 (log K_{app} = 17.2) that mediates peptide precipitation and that the tendency of this peptide to self-aggregate in aqueous solutions is due to the presence of trace Cu^{2+} contamination (customarily ~0.1 μ*M*). In contrast, Aβ1–40 has much lower affinity for Cu^{2+} at this site (estimated log K_{app} = 10.3), explaining why this peptide is less self-aggregating. The greater Cu^{2+}-binding affinity of Aβ1–42 compared with Aβ1–40 is associated with significantly diminished negative cooperativity. The role of trace metal contamination in inducing Aβ precipitation was confirmed by the demonstration that Aβ peptide (10 μ*M*) remained soluble for 5 days only in the presence of high-affinity Cu^{2+}-selective chelators. **Key Words:** Human amyloid β peptide—Copper—Affinity—Stoichiometry—Alzheimer's disease—Binding affinity method—Chelators.
J. Neurochem. **75,** 1219–1233 (2000).

Alzheimer's disease (AD) is characterized pathologically by the deposition of amyloid plaques and neurofibrillary tangles and by neuronal degeneration in the brains of affected individuals. Amyloid deposits are composed primarily of the amyloid β (Aβ) protein (Masters et al., 1985; Roher et al., 1996) generated as a mixture of polypeptides manifesting carboxyl- and amino-terminal heterogeneity. The Aβ1–40 isoform is the predominant soluble species in biological fluids (Shoji et al., 1992; Vigo-Pelfrey et al., 1993). Although less abundant in biological fluids, Aβ1–42 is the predominant species found in plaque deposits (Masters et al., 1985; Roher et al., 1996).

Metal ion homeostasis is severely dysregulated in AD (Hershey et al., 1983; Ehmann et al., 1986; Thompson et al., 1988; Vance et al., 1990; Basun et al., 1991; Samudralwar et al., 1995; Deibel et al., 1996; Cornett et al., 1998; Lovell et al., 1998; González et al., 1999). Although the transition metal ions Cu, Fe, and Zn are maintained at high concentrations within the healthy brain neocortical parenchyma (total dry weight concentrations of 70, 340, and 350 μ*M*, respectively), increased concentrations of these metal ions are detected in the neuropil of the AD-affected brain, where they are highly concentrated within amyloid plaque deposits with total concentrations reaching ~0.4 and ~1 m*M* for Cu and Fe/Zn, respectively (Lovell et al., 1998). An elevated Zn^{2+} concentration also can be detected in plaque deposits histologically (Suh et al., 2000). We previously found that Aβ avidly binds Cu^{2+}, Zn^{2+}, and Fe^{3+} (Bush et al., 1994*a*,*b*, 1995; Huang et al., 1997; Atwood et al., 1998), perhaps explaining the recruitment of these metals into amyloid plaque pathology.

Evidence for an interaction between Cu^{2+} and Aβ1–40 was first observed by the stabilization of an

Resubmitted manuscript received April 4, 2000; accepted April 18, 2000.

Address correspondence and reprint requests to Dr. A. I. Bush at Laboratory for Oxidation Biology, Genetics and Aging Unit, Neuroscience Center, Massachusetts General Hospital East, Building 149, 13th Street, Charlestown, MA 02129-9142, U.S.A. E-mail: bush@helix.mgh.harvard.edu

Drs. C. S. Atwood and R. C. Scarpa contributed equally to this article.

Abbreviations used: Aβ, amyloid β; AD, Alzheimer's disease; CDTA, *trans*-1,2-diaminocyclohexane-*N*,*N*,*N*′,*N*′-tetraacetic acid; CMCA, competitive metal capture analysis; DSA, dog serum albumin; DTPA, diethylenetriaminepentaacetic acid; PAGE, polyacrylamide gel electrophoresis; SDS, sodium dodecyl sulfate.

TABLE 1. *Log K_{app} of Cu^{2+}- and Zn^{2+}-selective chelators*

	Cu^{2+} log K_{app}				Zn^{2+} log K_{app}		
Chelator	pH 7.4	pH 7.0	pH 6.6	Chelator	pH 7.4	pH 7.0	pH 6.6
Tris	1.8	1.4	1.0	Tris	3.2	2.8	2.4
Glycine	5.9	5.5	5.1	Bicine	4.7	4.3	3.9
Arginine	5.9	5.5	5.1	Histidine	5.0	4.5	4.2
Methionine	6.3	5.9	5.5	ACES	5.0	4.6	4.2
Asparagine	6.6	6.2	5.8	Citric acid	5.3	4.9	4.5
Histamine	7.2	6.8	6.4	Bipyridyl	5.8	5.4	5.0
Bicine	7.4	7.0	6.6	Tricine	6.5	6.1	5.7
Ethylenediamine	7.8	7.4	7.0	HIMDA	7.1	6.7	6.3
Histidine	8.4	8.0	7.8	NTA	8.0	7.6	7.2
Bipyridyl	8.9	8.5	8.1	EGTA	10.0	9.6	9.2
HIMDA	10.6	10.2	9.8				
EDDA	14.1	13.7	13.3				
EDTA	15.9	15.5	15.1				
DTPA	16.3	15.9	15.5				
CDTA	17.0	16.6	16.2				

ACES, *N*-(carbamoylmethyl)-2-aminoethanesulfonic acid; bicine, *N,N*-bis(2-hydroxyethyl)glycine; bipyridyl, 2,2′-dipyridyl; EDDA, ethylenediamine-*N,N*′-diacetic acid; HIMDA, *N*-(2-hydroxyethyl)iminodiacetic acid; NTA, nitrilotriacetic acid; Tricine, *N*-tris(hydroxymethyl)methylglycine.

Determination of apparent log *K* from absolute log *K*

Metal ion chelators were chosen from the National Institute of Standards and Technology Standard Reference Database 46 (Critically Selected Stability Constants of Metal Complexes Database, version 4.0; U.S. Department of Commerce) and other reference databases (Dawson et al., 1986). Chelators were chosen to give a range of stability constants at approximately half log order intervals. Stability constants ($K = [ML]/[M][L]$, where M = metal ion and L = ligand) chosen for metal:chelators were for 25°C, an ionic strength of 0.1–0.2 υ, and a molar ratio of chelator to metal ion of 1:1. Where more than one complex is formed between a metal ion and a chelator, a chelator was only elected if the log K of its metal:chelator complex with a ratio of 1:1 was the greatest of all possible complexes.

The log K of a chelator for metal ions is affected by the pH of the solution as determined by the following equations [after Ringblom (1963) and Schwarzenbach and Flaschka (1969)]:

$$\log K_{\text{apparent}} = \log K - \log \alpha$$

where

$$\alpha = \frac{[H^+]_n}{K_{a1} * K_{a2} * K_{a3} * \ldots K_{an}} + \frac{[H^+]_{n-1}}{K_{a1} * K_{a2} * \ldots K_{an-1}} + \cdots + \frac{[H^+]}{K_{a1}} + 1$$

$K_a = 10^x$, where $x = -pK_a$ of the chelator (K_a values are listed in order of decreasing pK_a values), and n = no. of pK_a values. Values for log K_{app} for chelators used at pH 7.4, 7.0, and 6.6 are presented in Table 1.

Stoichiometry and binding analyses of metal ions for Aβ and DSA

Solutions of metal:chelator were prepared in a ratio of 1:2 (5 m*M*:10 m*M*) in doubly deionized water and allowed to come to equilibrium for 24 h at room temperature. Samples containing Aβ (10 μ*M*) or DSA (10 μ*M*) with and without metal ion: chelator complexes (50 μ*M* metal ion, 100 μ*M* chelator), along with background controls of protein plus chelator (no metal) or metal:chelator alone, were prepared in 20 m*M* Tris/150 m*M* NaCl buffer at pH 7.4 and 6.6 (for Aβ) and pH 7.0 (for DSA) to a final volume of 1 ml and incubated for 24 h at 37°C. Tris was chosen as the buffer because it only weakly complexes Cu ions and its log K_{app} has been characterized (Dawson et al., 1986). The value of pH 6.6 was chosen as a condition of severe acidosis and also to make comparisons with our previous publication.

Following incubation the sample was split into three fractions: Fraction 1 was used to confirm the initial concentrations of total protein [150 μl for Micro BCA assay (Pierce, Rockford, IL, U.S.A.)] and total metal ion (150 and 20 μl for Cu and Zn assays, respectively) in the reaction samples. Fraction 2 (330 μl) was loaded into a 3-kDa cutoff filter (Concentrator; Amicon, Beverly, MA, U.S.A.) and centrifuged at 10,000 *g* for 30–45 min, and the filtrate, which contained no peptide, was collected for metal ion analysis (20 μl for Zn and 160 μl for Cu). Fraction 3, the remainder of the reaction sample (330 μl), was centrifuged for 10 min at 10,000 *g*, and the supernatant was assayed for soluble protein and metal ion concentrations from which the respective concentrations in the pellet could be deduced. We have previously shown that centrifugation of Aβ solutions at 10,000 *g* for 10 min sediments all precipitated Aβ compared with ultracentrifugation at 100,000 *g* for 1 h (Atwood et al., 1998). As DSA did not precipitate in the presence of Zn^{2+} or Cu^{2+}, reaction mixtures of DSA and metal ions were divided into fractions 1 and 2 for assay. Appropriate blank samples (buffer with or without Aβ, buffer with or without metal ion) also were analyzed for background readings.

Scatchard analysis

Having assayed the amount of protein-bound metal ion in the incubation, the remaining metal ion in the non–protein-bound fraction is in an equilibrium between being free and being bound to the chelator. Therefore, the free concentration of metal ion could be calculated using the chelator stability constant for the metal ion applied to this fraction. Scatchard linearization analysis was only performed on data where the

gate by incubation in 20 m*M* Tris/150 m*M* NaCl buffer at pH 7.4 or 6.6 with $CuCl_2$ (20 μM) for 1 h at 37°C. Following precipitation, samples were incubated with no chelator, EDTA, or DTPA (200 μM each) for 1 h at 37°C. Samples were then centrifuged (10,000 *g* for 20 min), and the supernatant was analyzed for protein concentration to determine percent total peptide in the soluble fraction as previously described (Atwood et al., 1998).

Competition analyses of zinc and copper for Aβ

Aβ1–40 (10 μM) was incubated in 20 m*M* Tris/150 m*M* NaCl buffer at pH 7.4 or 6.6 with $ZnCl_2$, $Cu(NO_3)_2$, or $ZnCl_2$ plus $Cu(NO_3)_2$ (50 μM each) for 48 h or $ZnCl_2$ (50 μM) for 24 h, and then $Cu(NO_3)_2$ (50 μM) was added for a further 24 h. Following incubation, samples were analyzed for percent precipitation and stoichiometry of metal ion binding to Aβ as described above.

SDS-resistant polymerization of Aβ

Aβ stock solutions were diluted to 2.5 μM in phosphate-buffered saline (66 m*M* phosphate and 150 m*M* NaCl, pH 7.4) and incubated with or without $CuCl_2$ (30 μM) for 0 and 1 day at 37°C. Aliquots of each reaction mixture (2 ng of peptide) were collected into 15 μl of sample buffer (containing 4% SDS and 5% β-mercaptoethanol) and heated to 95°C for 5 min. Samples were loaded, electrophoresed on polyacrylamide gel electrophoresis (PAGE; Tricine gels, 10–20%; Novex, San Diego, CA, U.S.A.) at 25°C and pH 8.45, transferred to polyvinylidene difluoride membranes (Bio-Rad Laboratories, Hercules, CA, U.S.A.), fixed with glutaraldehyde (1%, vol/vol), blocked with milk (10%, wt/vol), and then probed with anti-Aβ monoclonal antibody 6E10 (or 4G8; Senetek, Maryland Heights, MI, U.S.A.) overnight at 4°C. The blot was then incubated with anti-mouse horseradish peroxidase conjugate (Pierce) for 2 h at room temperature and developed with ECL reagent (1 min; Amersham, Little Chalfont, Bucks, U.K.) or Supersignal Ultra (5 min; Pierce) following the manufacturer's instructions. The chemiluminescent signal was captured on film or for 10 min at maximal sensitivity using the Fluoro-S Image Analysis System (Bio-Rad). Electronic images were analyzed using Multi-Analyst Software (Bio-Rad). Molecular size markers were from Amersham (Arlington Heights, IL, U.S.A.).

RESULTS

Stoichiometry and estimated binding affinities of Cu^{2+} and Zn^{2+} for DSA

We developed a method (CMCA) to enable the determination of stoichiometry of metal ion binding to both soluble and precipitated forms of Aβ and to permit an estimation of metal ion binding affinities to Aβ (Fig. 1). To validate this methodology, we first studied a protein with known Cu^{2+} and Zn^{2+} binding affinities (DSA) (Fig. 2). DSA was found to bind on average ~2 Zn^{2+} (1.7 ± 0.2; mean ± SD) in the presence of Zn^{2+}:chelator complexes with log K_{app} values of ≤6.2 at pH 7.0 (Fig. 2A). Scatchard analysis of Zn^{2+} binding to DSA indicated that there was a single affinity binding site ($K_D = 1.3 \times 10^{-7}$ *M*, log $K_{app} = 6.9$) binding both Zn^{2+} ions (Fig. 2B), in agreement with previously reported values (Masuoka et al., 1993).

DSA also bound ~2 Cu^{2+} ions (1.7 ± 0.1; mean ± SD) when incubated in the presence of Cu^{2+}:chelator

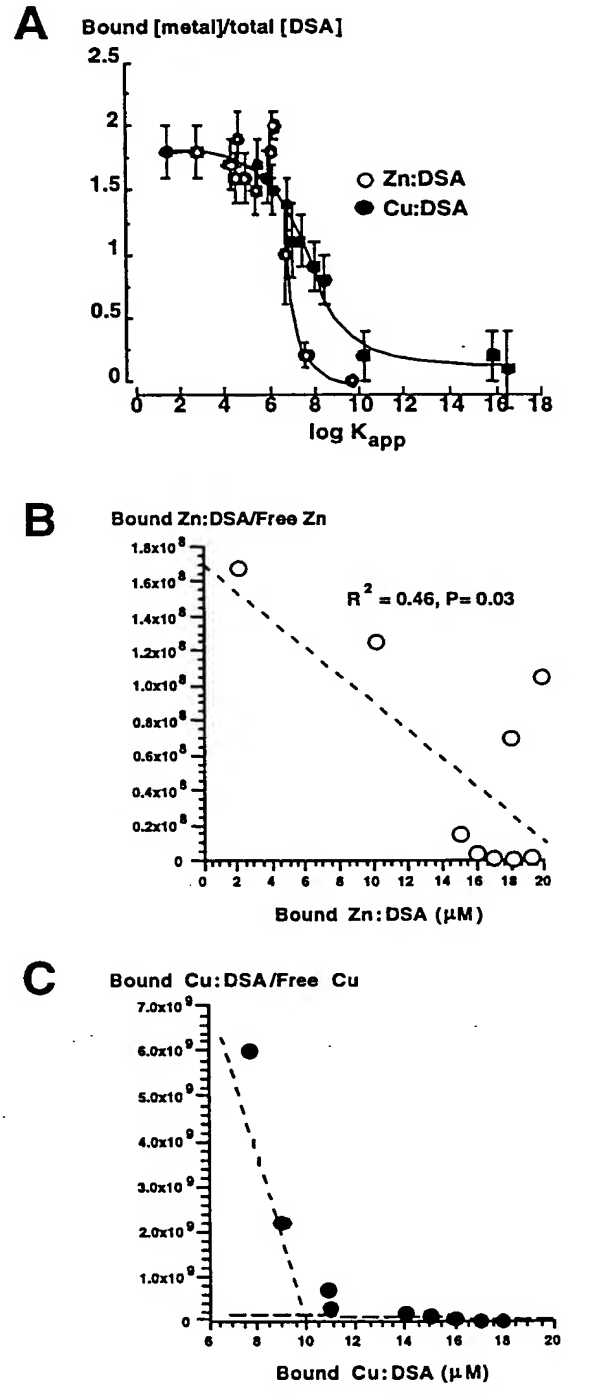

FIG. 2. CMCA of Cu and Zn binding to DSA. **A:** DSA (10 μM) was incubated with metal:chelator complexes (50 μM) for 24 h, and the stoichiometry of binding was determined. Data are mean ± SD (bars) values (n = 6). **B** and **C:** Scatchard analysis of the data in A.

TABLE 2. *Summary of binding affinities (log K_{app}) for Cu^{2+} binding to Aβ1–40 and Aβ1–42*

	Aβ1–40		Aβ1–42				
	log K_{app}	Stoichiometry of Cu:Aβ	log K_{app}	Stoichiometry of Cu:Aβ			
pH 7.4							
Highest affinity	10.3	0.5	17.2	0.5			
Lowest affinity	7.9	2	8.3	2			
	Slope [log(*B*/*F*)]/*B*	R^2	Slope [log(*B*/*F*)]/*B*	R^2	*t*	*df*	*p*
	−0.20	0.93	−0.50	0.88	2.98	44	0.002
pH 6.6							
Highest affinity	9.6	0.5	16.3	0.5			
Lowest affinity	7.0	2.5	7.5	2.5			
	Slope [log(*B*/*F*)]/*B*	R^2	Slope [log(*B*/*F*)]/*B*	R^2	*t*	*df*	*p*
	−0.15	0.92	−0.42	0.90	3.03	44	0.002

The data in Fig. 3 for Cu^{2+} binding to Aβ were analyzed and are summarized here. Log K_{app} values are derived from the slopes of the Scatchard plots in Fig. 3E, and the estimated stoichiometries of Cu^{2+} binding to the highest- and lowest-affinity sites are derived from the estimated *x*-axis intercepts in Fig. 3E. The slope of the analysis of [log(*B*/*F*)]/*B* derived from the insets of Fig. 3E is shown, along with the regression coefficients of these slopes, reflecting cooperative binding of Cu^{2+} to Aβ. The slope of [log(*B*/*F*)]/*B* for Cu^{2+} binding to Aβ1–42 is significantly greater than the slope of [log(*B*/*F*)]/*B* for Cu^{2+} binding to Aβ1–40 [*t* test value, degrees of freedom (*df*), and *p* values are shown]. This indicates that there is significantly greater cooperative binding of Cu^{2+} to Aβ1–42 compared with Aβ1–40.

plexes except in the presence of the chelator with the highest affinity for Cu^{2+} [*trans*-1,2-diaminocyclohexane-*N*,*N*,*N*′,*N*′-tetraacetic acid (CDTA), log K_{app} = 17.0], when the solubility of the peptide abruptly and dramatically increased (Fig. 3B). The possibility of CDTA directly binding to Aβ1–42 and acting as a chain breaker was excluded by nuclear magnetic resonance spectroscopy studies (X. Huang, K. Barnham, C. S. Atwood, R. E. Tanzi, and A. I. Bush, unpublished data).

At pH 6.6, the stoichiometry of low-affinity Cu^{2+} binding to both peptides increased (Fig. 3C). At pH 6.6, Aβ1–40 and Aβ1–42 bound 0.8 and 0.3 more Cu^{2+} ions (2.6 ± 0.1 and 2.5 ± 0.1, respectively) than at pH 7.4 in the presence of Cu^{2+}:chelator complexes in lower-affinity range (log K_{app} < 7.8), so that the stoichiometry of Cu^{2+} binding to Aβ1–40 approached that of Aβ1–42 (Fig. 3C). At pH 6.6, the affinity of the lowest-affinity Cu^{2+} binding site estimated by Scatchard analysis (Fig. 3E) decreased for both Aβ1–40 and Aβ1–42 (Aβ1–40, $K_D = 9.3 \times 10^{-8}$ *M*, log K_{app} = 7.0; Aβ1–42, $K_D = 3.3 \times 10^{-8}$ *M*, log K_{app} = 7.5; Table 2), compared with the affinity at pH 7.4. There was no significant change in Cu^{2+}:Aβ stoichiometry after incubation with Cu^{2+}:chelator complexes in the high-affinity range (log K_{app} = 7.8–16.2) at pH 6.6 compared with the values at pH 7.4. There was an accompanying decrease of ≈1 log unit in the estimated log K_{app} values for the high-affinity Cu^{2+} binding sites for both Aβ1–40 ($K_D = 2.6 \times 10^{-10}$ *M*, log K_{app} = 9.6; Table 2) and Aβ1–42 ($K_D = 4.5 \times 10^{-17}$ *M*, log K_{app} = 16.3; Table 2) at pH 6.6 (Fig. 3C and E), compared with the corresponding values at pH 7.4 (Fig. 3A and E).

The slope of the plot of log(bound [Cu^{2+}]/free [Cu^{2+}]) and bound [Cu^{2+}] (Fig. 3E, insets) correlates with the cooperativity coefficient for the multiple Cu^{2+} binding sites on Aβ. We found that at either pH 6.6 or 7.4, this slope was significantly (≈2.5-fold, $p = 0.002$) greater for Cu^{2+} binding to Aβ1–42 than for binding to Aβ1–40 (Fig. 3E and Table 2). This means that the acceleration of the Scatchard plot was 2.5-fold greater for Cu^{2+} binding to Aβ1–42, indicating that Aβ1–42 has markedly greater cooperative binding of Cu^{2+} than Aβ1–40.

The increase in low-affinity Cu^{2+} binding to Aβ1–40 induced by incubation at the lower pH (6.6) correlated with a ≈30% increase in Aβ1–40 precipitation (Fig. 3D) compared with that induced at pH 7.4 (Fig. 3B). However, although the incubation at pH 6.6 increased low-affinity Cu^{2+} binding to Aβ1–42, precipitation of Aβ1–42 at the lower pH (Fig. 3D) was not increased compared with precipitation at pH 7.4 (Fig. 3B).

Although at pH 7.4 CDTA did not permit sufficient Cu^{2+} to bind to Aβ1–42 to induce peptide precipitation (Fig. 3B), at pH 6.6 incubation of Aβ1–42 with CDTA:Cu^{2+} complexes was accompanied by ≈50% precipitation of Aβ1–42 (Fig. 3D). Note, however, that CDTA and all of the chelator array have lower Cu^{2+} binding affinities at the lower pH; the log K_{app} of CDTA for Cu^{2+} decreases from 17.0 at pH 7.4 to 16.2 at pH 6.6 (Table 1).

Taken together, these findings indicate that Aβ1–40 and Aβ1–42 precipitate if bound to 1 Cu^{2+}. Conversely, Aβ1–40, and even Aβ1–42 (at pH 7.4), will remain soluble if Cu^{2+} binding is totally prevented.

Although there was a strict correspondence between the stoichiometry of bound Cu^{2+} and the amount of Aβ1–40 precipitation (r^2 = 0.89 at pH 7.4 and 0.85 at pH 6.6; Fig. 4), there was a weak correlation (and at pH 6.6, no correlation) between the stoichiometry of bound Cu^{2+} and the amount of Aβ1–42 precipitation (r^2 = 0.17 at pH 7.4 and r^2 = 0.09 at pH 6.6; Fig. 4). The change in pH from 7.4 to 6.6 did not alter the slope of the linear relationship between Cu^{2+}:Aβ1–40 stoichiometry and precipitation (Fig. 4), which indicates that the Cu^{2+} binding to Aβ1–40 saturates at 2.5 Cu^{2+} ions.

TABLE 4. *Competition between Cu^{2+} and Zn^{2+} for metal ion binding sites on Aβ1–40 at pH 7.4 and 6.6*

	pH 7.4	pH 6.6
Zn^{2+} + Aβ, 48 h		
% precipitation	88.4 ± 0.9	85.0 ± 0.4[a]
Ratio Zn:Aβ	2.88 ± 0.03	2.03 ± 0.19[a]
Cu^{2+} + Aβ, 48 h		
% precipitation	58.0 ± 3.9	85.4 ± 6.0[a]
Ratio Cu:Aβ	1.91 ± 0.15	2.76 ± 0.10[a]
Zn^{2+} + Cu^{2+} coincubated for 48 h		
% precipitation	79.0 ± 3.8	64.0 ± 7.2[b]
Ratio Zn:Aβ	1.90 ± 0.18	0.33 ± 0.09[a]
Ratio Cu:Aβ	1.68 ± 0.09	3.13 ± 0.05[a]
Total metal:Aβ ratio	3.58	3.46
Zn^{2+} for 24 h, then Cu^{2+} for 24 h		
% precipitation	65.8 ± 7.2	82.0 ± 4.1[a]
Ratio Zn:Aβ	1.74 ± 0.29	0.67 ± 0.22[a]
Ratio Cu:Aβ	1.48 ± 0.09	2.75 ± 0.04[a]
Total metal:Aβ ratio	3.22	3.22

The following incubations were done: (a) Aβ1–40 was incubated with 50 μM Zn^{2+} for 48 h; (b) Aβ1–40 was incubated with 50 μM Cu^{2+} for 48 h; (c) Aβ1–40 was incubated with 50 μM Zn^{2+} and 50 μM Cu^{2+} for 48 h; or (d) Aβ1–40 was incubated with 50 μM Zn^{2+} for 24 h, 50 μM Cu^{2+} was added, and the mixture was incubated for a further 24 h. Stoichiometry represents metal ion binding to total (precipitated and soluble) Aβ1–40. All experiments were done in Tris-buffered saline. Data are mean ± SD values (n = 6).

The statistical significance of comparisons between pH 7.4 and 6.6 for percent precipitation and ratio of metal:Aβ for each experiment was determined by *t* test (two-tailed, heteroscedastic): [a]$p < 0.001$, [b]$p < 0.005$.

though the aggregated Aβ1–42 bound 0.7 more Cu^{2+} at pH 6.6 than at pH 7.4.

Cu^{2+} initiates the nucleated precipitation of Aβ1–40 and Aβ1–42

Because, unlike Aβ1–40, the precipitation of Aβ1–42 did not correlate with the stoichiometry of bound Cu^{2+}, we studied the possibility that the precipitation of Aβ1–42 was by a seeding mechanism (Jarrett et al., 1993) where Cu^{2+} initiates peptide nucleation but that the precipitation of the majority of the solution was not metal-dependent. First, we measured the amount of precipitation of Aβ in the absence of added metal ions or chelators, incubated for 24 h under the same conditions as Fig. 3 and Table 3. The precipitation of Aβ1–40 and Aβ1–42 formed by an apparent seeding mechanism in the absence of metal ions or chelators was greater at pH 6.6 (23 ± 7 and 95 ± 4%, respectively) than at pH 7.4 (10 ± 2 and 87 ± 1%), in agreement with our previous report (Atwood et al., 1998). It is surprising that the precipitation of Aβ1–40 or Aβ1–42 at pH 6.6 in the absence of added metal ions was greater than the corresponding amount of Aβ1–40 or Aβ1–42 precipitation that occurred in the presence of 50 μM Cu^{2+} that had been complexed with any of the high-affinity chelators (log $K_{app} \geq 10.6$; Fig. 3B and D). To illustrate this, in Fig. 5A we compare the precipitation of Aβ1–40 and Aβ1–42 in the presence and absence of the DPTA:Cu^{2+} complex. We studied DTPA because NMR spectroscopy of DTPA coincubated with Aβ1–40 and Aβ1–42 indicated that the chelator does not bind to the peptide (X. Huang, K. Barnham, C. S. Atwood, R. E. Tanzi, and A. I. Bush, unpublished data); hence, any effect of DTPA in preventing Aβ precipitation is not due to β-sheet chain breaking. We observed that there is more precipitation of either Aβ1–40 or Aβ1–42 in the absence of added metal ions than in the presence of DPTA:Cu^{2+} complexes, at either pH (Fig. 5A). This indicates that the increased precipitation of Aβ at pH 6.6 in the absence of added metal ions could not be explained by pH effects alone and suggests that trace metal ion contamination of the buffers mediates the apparent seeding of Aβ solutions. Supporting this possibility, we measured the contaminating concentration of Cu^{2+} in buffer solutions containing Aβ as ~0.1 μM, using inductive coupled plasma mass spectrometry.

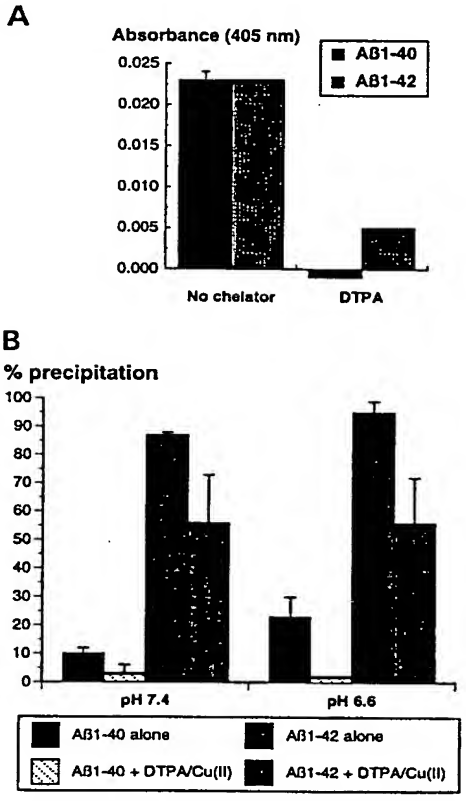

FIG. 5. Inhibition of Aβ nucleated precipitation by DTPA. **A:** Aβ1–40 or Aβ1–42 (10 μM) was incubated at pH 7.4 and 6.6 with or without Cu^{2+}:DTPA complex (chelator complex data selected from Fig. 3B and D) for 24 h, and precipitation was determined as in Fig. 3. Data are mean ± SD (bars) values (n = 6). **B:** Aβ1–40 or Aβ1–42 (10 μM each) was incubated in phosphate-buffered saline (pH 7.4) with or without DTPA (200 μM) for 5 days at 37°C. Precipitation was assessed by measuring the turbidity of the solution at 405 nm. Data are mean ± SD (bars) values (n = 4).

DISCUSSION

CMCA

The CMCA technique was developed for the practical assessment of stoichiometry and affinities of metal ion binding to soluble and precipitated proteins. Validation of our methodology was obtained by a comparison of Cu^{2+} and Zn^{2+} binding affinities with the known affinities for DSA (Fig. 2). This technique circumvents several problems associated with preexisting methodologies for the assessment of metal ion binding to proteins. Competition studies often require the use of expensive and hazardous radioactive metal ions or ligands, and spectrophotometric or fluorescence techniques lack sensitivity in the submicromolar metal ion concentration range and rely on conformational changes in the target protein.

Despite these advantages, the CMCA method relies on the availability of an array of chelators that reflect log K_{app} values within the range of interest. To this end, we attempted to provide chelators at log K_{app} intervals of no more than 0.5 units, but the number of usable chelators with log $K_{app} > 10$ was small. The array of data points required by this technique should be improved as we identify further appropriate chelators for use in the assay.

Binding interactions with Cu^{2+} differentiate Aβ1–40 and Aβ1–42

Our current results, summarized in Table 2, indicated multiple affinity Cu^{2+} binding sites on Aβ1–40 and Aβ1–42 that were considerably greater than the single affinities (4.0 and 0.3 μM, respectively) initially obtained for the peptides using spectrophotometric analysis (Atwood et al., 1998). This apparent discrepancy is probably because, in the previous study, the precipitation of the peptide by Cu^{2+} withdrew a fraction of the peptide from spectral analysis and may have artifactually lowered the sensitivity of the technique to detect physicochemical changes. Also, the spectrometric analysis we used previously would have been only capable of appreciating spectral shifts associated with saturation of the lower-affinity Cu^{2+} binding site on Aβ. This is because in our previous analysis we measured the spectroscopic response of synthetic peptide to increments of ≥ 0.1 μM in Cu^{2+} concentration. Because the background contamination of the incubation buffer with Cu^{2+} is ~ 0.1 μM and because we have now identified Cu^{2+} binding sites on Aβ with subnanomolar affinities, the previous technique could not have reliably titrated the Cu^{2+} concentration in low nanomolar increments to appreciate a consequent spectroscopic effect. An advantage of the current CMCA technique was that we could titrate the physicochemical effects of the exchange of Cu^{2+} to Aβ against the known binding affinities of chelators in competition for Cu^{2+}, without the need to titrate metal ion concentrations that are below background contamination levels.

The estimated log K_{app} for the Cu^{2+} binding site on Aβ1–42 (log K_{app} = 17.2; Table 2) translates into a predicted affinity for Cu^{2+} in the attomolar range and for Aβ1–40 in the picomolar range (estimated log K_{app} = 10.3; Table 2), indicating that Cu^{2+} could be bound to Aβ (Aβ1–42 ≫ Aβ1–40) under biological conditions. Also, the concave acceleration of the Scatchard analyses of Cu^{2+} binding to Aβ1–40 and Aβ1–42 (Fig. 3E) suggests negative cooperativity of the binding sites. Aβ1–42 was found to have significantly less hindrance in binding successive Cu^{2+} ions compared with Aβ1–40. Aβ1–42 also exhibits higher affinity Cu^{2+} binding than Aβ1–40 at both the lowest- and highest-affinity binding sites observed, which indicates that the structural basis for Cu^{2+} binding and the allosteric basis for cooperativity may be mediated by the hydrophobic carboxyl-terminal tail of Aβ. Aβ1–42 reportedly has a higher β-sheet content than Aβ1–40 (Barrow et al., 1992), and β-sheet or β-barrel conformations are known to mediate other high-affinity Cu binding sites (Fraústo da Silva and Williams, 1993). The increased β-sheet content of Aβ1–42 makes the peptide more liable to self-associate and to precipitate (Jarrett et al., 1993). This self-association could have an allosteric impact on Cu^{2+} binding, especially if Cu^{2+} binding to Aβ involves multmeric interactions between protein subunits, It is also possible that nucleated precipitation of Aβ1–42 (see below) may have perturbed the equilibrium of bound to free soluble Cu^{2+} as the Cu^{2+} is removed from the soluble phase, thus contributing to the log K_{app} value we have observed. However, the possibility of irreversible withdrawal of Cu^{2+} associated with the precipitating peptide was not supported by our observation that high-affinity Cu chelators resolubilized Cu^{2+}-associated Aβ1–42 deposits (Fig. 6). It is also unlikely that our results only reflect Cu^{2+} binding to preassociated Aβ because the precipitation of soluble Aβ in the presence of Cu^{2+} occurs within seconds (Atwood et al., 1998) but over days in the absence of added metal ions (Jarrett et al., 1993). Nevertheless, preliminary data indicate Cu^{2+} binds to fibrillized Aβ with approximately the same stoichiometry as to fresh soluble Aβ (C. S. Atwood et al., unpublished data).

The structures of the multiple Cu^{2+} binding sites on soluble and precipitated Aβ are not yet clear and could be complex because new sites may form during the assembly of the peptide. Some evidence suggests that Aβ forms a dimer in solution (Garzon-Rodriguez et al., 1997; Huang et al., 1997). Therefore, the noninteger stoichiometry of 0.5 equivalents that was clearly observed for the highest-affinity binding site on Aβ1–42 and 2.5 equivalents for the lowest-affinity Cu^{2+} binding site on both Aβ1–40 and Aβ1–42 at pH 6.6 (Fig. 3E and Table 2) may reflect interaction with Aβ dimers. It is also possible that some binding sites are created by residues on neighboring Aβ subunits that are only brought into Cu^{2+}-coordinating alignment as the peptide aggregates.

We have also shown for the first time that Cu^{2+} slowly modifies Aβ, inducing SDS resistance (Fig. 7). Previous studies have shown that Fe/H_2O_2 oxidation systems promote SDS-resistant polymerization of Aβ generated in a wheat germ expression system (Dyrks et al., 1992), but

deprotonates and selectively coordinates to Cu^{2+}. Our recent electron paramagnetic resonance evidence has indicated a coordination sphere for Cu^{2+} to Aβ of CuN_3O_1 (Huang et al., 1999*b*), and detailed simulations reveal that only two of these nitrogens are His residues, whereas the third is a deprotonated amide-N. When Cu^{2+} coordinates to an amide nitrogen, it is able to increase dramatically the acidity of the amide NH to <7 and as low as 4, whereas the pK_a of amides bound to Zn^{2+} is still ~12 (Sigel and Martin, 1982). This selective stabilization of a deprotonated (anionic) amide is the result of more effective ligand-to-metal charge transfer from the deprotonated amide nitrogen to the d^9 Cu^{2+} versus a d^{10} Zn^{2+} transition metal ion. This is a common phenomenon among other electrophilic transition metal ions with vacant *d* orbitals (Woon and Fairlie, 1992). Therefore, we propose that although His residues may contribute to the coordination of both Cu^{2+} and Zn^{2+} sites, one amide group may coordinate an additional low-affinity Cu^{2+} as the pH is lowered from 7.4 to 6.6, whereas high-affinity Cu^{2+} coordination and Zn^{2+} coordination may be simultaneously weakened. A similar increase in Cu^{2+} binding in response to acidic pH (pH 3–6) has recently been reported for the multicopper oxidase apoFet3p (Davis-Kaplan et al., 1998).

Possible physiological and pathological roles for the selective Cu^{2+} and Zn^{2+} binding sites on Aβ

Our data indicate that Aβ binds approximately equivalent amounts of Cu^{2+} and Zn^{2+} at pH 7.4 but that Cu^{2+} totally displaces Zn^{2+} binding to Aβ at pH 6.6. We have previously published the finding that at pH 7.4 the Zn^{2+} binding site is very highly selective for Zn^{2+} and that at pH 7.4 Zn^{2+} cannot be displaced from binding Aβ by overwhelming concentrations of Cu^{2+} or any other transition metal ion (Bush et al., 1994*a*). Taken together with our current results, we hypothesize that Aβ possesses highly selective Cu^{2+} and Zn^{2+} binding sites at pH 7.4 but that at pH 6.6 there is a weakened affinity for Zn^{2+} but a preserved affinity for Cu^{2+} that allows the peptide to become occupied by Cu^{2+} at both sites. Thus, excessive Cu^{2+} binding of Aβ may be a consequence of mild acidosis and may have a deleterious promoting effect on the aggregation and the redox activities (Huang et al., 1999*a*,*b*; present study, Fig. 7) of the protein.

Low-affinity metal binding sites on Aβ mediate aggregation and precipitation and also may mediate Cu^{2+} reduction, O_2-dependent H_2O_2 production (Huang et al., 1999*a*), and oxidative modification of Aβ (Fig. 7). It is possible that one of the low-affinity Cu^{2+} sites we have observed may be due to Cu^{2+} occupying the Zn^{2+} site on Aβ. Abnormal Cu^{2+} binding to the Zn^{2+} binding site on wild-type and mutant superoxide dismutase has been shown to alter the redox chemistry of this protein and to promote radical generation, which may play a pathogenic role in familial amyotrophic lateral sclerosis (Goto et al., 1998). We contemplate similarities between this abnormal neurochemistry in familial amyotrophic lateral sclerosis and abnormal Aβ–metal interactions in AD.

Abnormal Cu/Zn interactions with Aβ in AD

Zn and Cu ions mediate the precipitation of Aβ deposits in AD brain as evidenced by the solubilization of Aβ from postmortem AD brain tissue that is promoted by chelators selective for these metals (Cherny et al., 1999) and also evidenced by the marked enrichment of total Cu and Zn in AD neuropil and amyloid plaques (Lovell et al., 1998), which could be explained by the high affinity of these metal ions for Aβ (present study, Fig. 3 and Table 2; Bush et al., 1994*a*; Atwood et al., 1998). It is not yet clear whether abnormal Cu (or Zn) homeostasis initiates Aβ deposition, or whether the accumulation of Aβ acts as a sink that draws metal ions into its mass. Significant increases in the concentration of Cu in the CSF [2.2-fold (Basun et al., 1991)] accompanied by an increase in level of CSF and brain ceruloplasmin, a Cu transport protein, in AD patients (Loeffler et al., 1994) further indicate that Cu homeostasis is compromised in AD.

Both Cu and Zn are released from vesicles of neurons during synaptic transmission reaching concentrations as high as 15 μ*M* (Hartter and Barnea, 1988) and 300 μ*M* (Frederickson, 1989), respectively. The proportion of binding of Cu and Zn to Aβ will depend on the respective stability constants of each metal ion for different ligands, their total concentrations, and the pH of the microenvironment. The release of Cu and Fe from metalloproteins is usually promoted by mildly acidic environments (reviewed by Atwood et al., 1998). However, under mildly acidic conditions Cu^{2+} binding to Aβ was enhanced, almost completely displacing Zn^{2+} from Aβ (Table 3). This unusual property of Aβ to accept Cu^{2+} under mildly acidic conditions, where most proteins lose metal ions with decreasing pH, may be important in the pathophysiology of AD, where metabolic compromise may result in acidosis (Yates et al., 1990).

Acknowledgment: The authors thank Diane Cabelli, Alan Kay, J. D. Robertson, and Kevin Barnham for helpful discussions. This work is supported by funds from the National Institutes of Health (grant R29AG12686), PRANA Corp., and the American Health Assistance Foundation.

REFERENCES

Appleton D. W. and Sarkar B. (1971) The absence of specific copper (II)-binding site in dog albumin. *J. Biol. Chem.* **246**, 5040–5046.

Atwood C. S., Moir R. D., Huang X., Bacarra N. M. E., Scarpa R. C., Romano D. M., Hartshorn M. A., Tanzi R. E., and Bush A. I. (1998) Dramatic aggregation of Alzheimer Abeta by Cu(II) is induced by conditions representing physiological acidosis. *J. Biol. Chem.* **273**, 12817–12826.

Barrow C. J., Yasuda A., Kenny P. T., and Zagorski M. G. (1992) Solution conformations and aggregational properties of synthetic amyloid beta-peptides of Alzheimer's disease. Analysis of circular dichroism spectra. *J. Mol. Biol.* **225**, 1075–1093.

Basun H., Forssell L. G., Wetterberg L., and Winblad B. (1991) Metals and trace elements in plasma and cerebrospinal fluid in normal

Soto C., Brañes M. C., Alvarez J., and Inestrosa N. C. (1994) Structural determinants of the Alzheimer's amyloid β-peptide. *J. Neurochem.* **63**, 1191–1198.

Spiro T. G. and Saltman P. (1969) *Structure and Bonding, Vol. 6.* Springer-Verlag, New York.

Suh S. W., Jensen K. B., Jensen M. S., Silva D. S., Kesslak J. P., Danscher G., and Frederickson C. J. (2000) Histological evidence implicating zinc in Alzheimer's disease. *Brain Res.* **852**, 274–278.

Thompson C. M., Markesbery W. R., Alaudin M., Hossain T. I. M., and Brubaker E. H. (1988) Regional brain trace-element studies in Alzheimer's disease. *Neurotoxicology* **9**, 1–8.

Vance D. E., Ehmann W. D., and Markesbery W. R. (1990) A search for longitudinal variations in trace element levels in nails of Alzheimer's disease patients. *Biol. Trace Element Res.* **26–27**, 461–470.

Vigo-Pelfrey C., Lee D., Keim P., Lieberburg I., and Schenk D. B. (1993) Characterization of β-amyloid peptide from human cerebrospinal fluid. *J. Neurochem.* **61**, 1965–1968.

Woon T. C. and Fairlie D. P. (1992) Amide complexes of diethylenetriamineplatinum(II). *Inorg. Chem.* **31**, 4069–4074.

Yates C. M., Butterworth J., Tennant M. C., and Gordon A. (1990) Enzyme activities in relation to pH and lactate in postmortem brain in Alzheimer-type and other dementia. *J. Neurochem.* **55**, 1624–1630.